PRINCIPLES OF CLINICAL NUCLEAR MAGNETIC RESONANCE IMAGING AND SPECTROSCOPY

Craig R. Malloy, M.D.

Medical Grand Rounds

University of Texas Health Science Center at Dallas

May 2, 1985

PRINCIPLES OF CLINICAL NUCLEAR MAGNETIC RESONANCE IMAGING AND SPECTROSCOPY

Craig R. Malloy, M.D.

PRINCIPLES OF CLINICAL NUCLEAR MAGNETIC RESONANCE IMAGING AND SPECTROSCOPY

Nuclear magnetic resonance (NMR) imaging is a powerful diagnostic technique that will become progressively more important to the practice of internal medicine. Application of NMR spectroscopy to metabolic studies has also broadened dramatically in the clinically-related basic sciences, and it is likely that NMR spectroscopy will have direct clinical application in the near future. The reader is certainly aware that there is hardly a general medical or biological journal that has not recently published articles regarding one aspect or the other of NMR. However, the fundamental principles that apply to both NMR imaging and spectroscopy are seldom emphasized. An appreciation of these principles may be useful to the internist for several reasons. The interpretation of any NMR study (spectroscopy or imaging) depends directly upon a clear understanding of the physical principles of NMR. This statement probably applies more to NMR imaging than to any other imaging technique. Second, certain concepts that are central to NMR theory and apply to any NMR study may be better illustrated by examples from imaging or spectroscopy. Finally, the evolution of NMR imaging and spectroscopy for clinical use will be to some degree convergent. Even if classical NMR spectroscopy never achieves widespread clinical utility, concepts that are "spectroscopic" will significantly influence the development of clinical NMR imaging.

Examples of the current state of clinical NMR imaging and spectroscopy are provided by the histories of two patients.

> A 30-year-old woman presented with a four year history consistent with temporal lobe seizures. There were no focal neurological findings. An x-ray computed tomogram (CT) showed a cystic structure in the right temporal lobe. The abnormality was interpreted as a benign cyst. The patient was followed with CT for two years. She was referred for an NMR study when it became available. Again, a cystic structure that appeared multiloculated was identified. However, images that emphasize T_1 dependent contrast indicated that the cyst did not contain normal cerebrospinal fluid. The NMR study indicated that the fluid filling the cavity contained a high concentration of protein. The structure was surgically removed because it was no longer considered benign. It was an astrocytoma. This case history was provided by Dr. Ken Maravilla.
>
> A 51-year-old man complained of a long history of fatigue after minimal exertion. He occasionally passed dark urine after extreme exertion. The family history was negative for similar complaints. Neurological exam was unremarkable; there was no muscle wasting or weakness. Serum creatine kinase and aldolase were elevated, and the electromyogram showed mild abnormality of the action potential. A histochemical exam of a muscle biopsy showed increased glycogen content and decreased phosphorylase activity. ^{31}P NMR study of the forearm muscles showed a mild intracellular alkalosis and normal relative concentrations of ATP, phosphocreatine, and inorganic phosphate. During exercise the [phosphocreatine] decreased more rapidly than in normal volunteers, and the usual intracellular acidosis associated with exercise was not observed (Figure 1). These results were indicative of a disorder reducing flux through glycolysis (because there was no change in muscle pH during exercise) and reduced ATP generation during exercise (138).

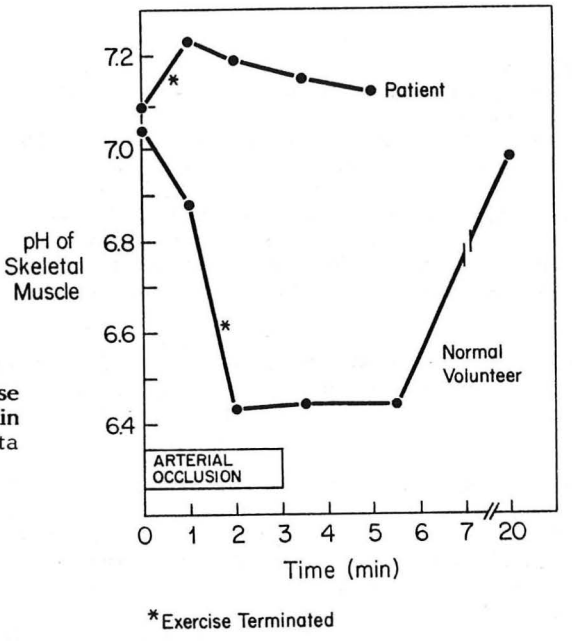

Figure 1. Influence of ischemic exercise on skeletal muscle intracelluar pH in a patient with McArdle's syndrome. Data from reference 138.

These histories demonstrate that NMR is a flexible technique for obtaining high quality diagnostic images and for providing insight into the metabolic state of tissue by non-invasive measurement of the relative concentrations of phosphates and pH. The basic principles of both techniques are the same. For certain clinical problems NMR imaging is already the favored imaging method, and for a much larger number of problems it provides information that complements standard methods. In contrast, the role of clinical NMR spectroscopy is currently much less significant than that of NMR imaging. However, NMR spectroscopy provides information that is difficult or impossible to obtain by other methods. Thus, the unique powers of NMR spectroscopy will be applied to clinical and animal research in most areas of internal medicine.

Objectives

The objectives of this review are three-fold. I intend to describe the physical basis of NMR with emphasis on those principles common to NMR imaging and spectroscopy. These principles will be developed further as they are applied specifically to NMR imaging or spectroscopy. Finally, I hope to illustrate these principles by examining results of selected patient studies. There is little emphasis on technical detail or financial considerations since this information is easily available in the literature or from manufacturers (23,24,52,57,59,62,91,107,132,134,140-142).

Terminology

Nuclear magnetic resonance is a physical phenomenon that may be used to generate images of patients (NMR imaging) or to obtain information about the structure and concentration of certain molecules in tissues of patients (NMR spectroscopy). There is apparently some aversion to using the word "nuclear" (45,112). The alternatives from which we may select include MRT (magnetic resonance tomography), CMR (clinical magnetic resonance), MRI (magnetic resonance imaging), and zeugmatography. MRI is recommended by the American College of Radiology. The event, nuclear resonance in a magnetic field, observed during any type of medical NMR study is identical to the event observed 40 years ago during the first NMR experiments. Thus, "nuclear magnetic resonance" is a well-established phrase that simply and accurately describes the general phenomenon. "MRI" has the advantage of specifically indicating ^{1}H NMR imaging.

Two phrases, "proton magnetic resonance" and "proton imaging" refer to NMR spectroscopy and imaging of hydrogen, ^{1}H. Although these phrases are not strictly correct (protons are present in other nuclei), they are encountered in the literature and in this review.

There are two measurements that are fundamental to any NMR discussion. The magnetic field is reported in units of Tesla or Gauss. One Tesla is 10,000 G. The standard unit is Tesla, abbreviated T. Frequency is reported in megahertz (MHz) or millions of cycles per second. The frequencies that apply to any medical NMR observation is in the range of radiofrequency (r.f.) waves, about 1-100 MHz.

2. PHYSICAL PRINCIPLES OF NUCLEAR MAGNETIC RESONANCE

The nuclei of many atoms may be considered as small magnets spinning on their axis. If a group of identical magnetic nuclei are placed in a magnetic field, then the axis of those nuclei will tend to align with the imposed field. In a similar manner, the needle of a compass aligns with the earth's magnetic field. If those nuclei are exposed to electromagnetic energy at exactly the right frequency, energy will be absorbed. A physical analogy is the response of a tuning fork to exactly the right frequency: it will absorb energy, or vibrate. The absorbed energy shifts the average orientation of the nuclei relative to the main field. Because these small magnets are spinning and tilted relative to the main field, they will move or precess around the axis of the main field. This phenomenon is similar to the precession of a gyroscope in the earth's gravitational field. Precession of the nuclei may be detected by an antenna. This is analogous to moving a magnet near a loop of wire which generates a current that can be detected.

This process applies equally to the phosphorus spectra and hydrogen images. It should be emphasized that this process is unrelated to administering or detecting ionizing radiation. The following is a more detailed review of NMR phenomena emphasizing those principles common to imaging and spectroscopy.

2.1 Classical Description of the NMR experiment

The sample: properties of nuclei that influence detection by NMR.

All nuclei may be characterized for our purposes by two numbers: I (spin) and γ (magnetogyric ratio). These numbers for certain elements and their isotopes are summarized in Table 1. Both I and γ significantly influence detection of an NMR signal.

The nuclei of all elements and their isotopes may be divided into two classes: those with a property conveniently called spin, and those without. Since all nuclei are charged, a spinning nucleus is effectively a moving charge. This moving charge generates a small magnetic field. These nuclei may be considered small spinning bar magnets. This property, spin, is independent of an imposed magnetic field, but it is essential for the detection of an NMR signal. The other number, magnetogyric ratio (γ), is essentially the ratio of magnetism of a nucleus to its mass. The higher the number the more efficiently the nucleus interacts with a magnetic field.

The type of information obtained from any NMR observation is determined primarily by the nucleus selected for detection, e.g., ^{1}H, ^{23}Na, or ^{31}P. Three factors determine which nuclei are available for observation. The relative sensitivity to the NMR experiment is different for different nuclei. For example, it is much easier to detect sodium in a 100 mM solution than it is to detect potassium at the same concentration. The sensitivity of any nucleus is described relative to ^{1}H under standard conditions. The relative sensitivity is proportional to $\gamma^3 I\,(I+1)$, where I is the spin of a nucleus and γ is the magnetogyric ratio. These numbers are determined by the number of protons and neutrons in the nucleus and are different for each isotope. Spin ranges from 0 to 9/2. For those nuclei with I = 0, an NMR signal cannot be detected because the nucleus cannot effectively interact with an applied magnetic field.

TABLE 1

NMR PROPERTIES OF SELECTED NUCLEI

Isotope	Natural Abundance*	Concentration in Tissue (M)	Relative Sensitivity**	Spin (I)	γ (MHz/T)
^{1}H	0.9998	66	1.00	$\frac{1}{2}$	42.6
^{2}H	0.0002	0	0.01	1	6.5
^{12}C	0.99	0.1	0	0	0
^{13}C	0.01	0	0.016	$\frac{1}{2}$	10.7
^{16}O	0.9996	33	0	0	0
^{19}F	1.00	0	0.83	$\frac{1}{2}$	40.0
^{23}Na	1.00	0.1	0.10	3/2	11.3
^{31}P	1.00	0.02	0.07	$\frac{1}{2}$	17.2
^{39}K	0.9310	0.1	0.0005	3/2	2.0

*Natural abundance refers to the proportion of the naturally occurring element that consists of the isotope of interest.

**Relative sensitivity refers to the sensitivity of that nucleus to the NMR experiment, compared to hydrogen at the same field and number of nuclei.

The second factor that influences detection of an isotope is the natural abundance. Many of the elements that make up human tissues are not "pure". For example, most of the chloride ions in the body are ^{35}Cl but a significant number are ^{37}Cl. Natural abundance refers to the proportion of the naturally-occurring element that consists of the isotope of interest.

Finally, the concentration of the isotope of interest in human tissue must be estimated. This concentration reflects the concentration of nuclei in a freely-diffusing molecule. For reasons beyond the scope of this discussion nuclei in molecules that are immobilized (e.g., bound to large proteins) are not easily detected by NMR.

These principles may be applied to the biologically-relevant nuclides. Water (H_2O) may contain one of two isotopes of hydrogen. The vast majority of hydrogen atoms in tissue are ^{1}H. A very few are ^{2}H, deuterium. This is fortunate because ^{1}H is an excellent nucleus for observation by NMR (Table 1). Most of the oxygen atoms, on the other hand, cannot be detected at all by NMR because the nucleus has no spin. Thus, even though the nucleus is present in the body at very high concentrations, it cannot be detected by NMR. Carbon is similar. Most of the nuclei in the body are ^{12}C which cannot be detected. However, a ^{13}C labelled substance can be administered to an animal, and metabolites may be detected. Sodium has a high natural abundance, a reasonable concentration in the body, and relatively poor sensitivity. Nevertheless, it is detectable by NMR and may prove to be a very important nucleus for imaging. For phosphorus, the situation is worse because the concentration in the body and the sensitivity of the nucleus are both rather poor, even though the nucleus is 100% abundant.

Thus, the magnetic properties of each isotope are distinctive. A crude summary of the technical suitability of a nucleus for NMR observation is the product of natural abundance, concentration in tissue, and relative sensitivity. This product may be compared to the result for ^{1}H.

The hydrogen nucleus is the nucleus of choice for imaging (at least "anatomic" imaging) because it possesses optimal properties: it is present in the body at very high concentration, it is nearly 100% naturally abundant, and it possesses excellent sensitivity. From these considerations, it is clear that detecting a signal from ^{23}Na or ^{31}P will be at the least associated with significant limitation of signal.

The Sample in a Magnetic Field

If a group of nuclei with non-zero spin is placed in a magnetic field, then the nuclei will tend to align with the magnetic field. The individual nuclei do not align exactly parallel with the applied field, but at an angle. Each nucleus precesses around the axis of the applied field, which is conventionally considered the z axis. The frequency of this precession, ν, depends on two factors: the specific nucleus being observed and the intensity of the magnetic field around the nucleus, B_L (B_{local}).

$$\nu = \gamma B_L \qquad [1]$$

The field applied by the magnet is B_0. Because of certain sample or experimental effects the nucleus experiences a slightly different field, B_L. The magnetogyric ratio, γ, is a unique constant for any nucleus with non-zero spin. The magnetic field and frequency of precession are proportional to one another, and the constant of proportionality is γ. It is very important to appreciate that γ is constant for a given nuclear isotope. In other words, for ^{1}H γ is about 43 MHz/T, and this value

is the same for ^1H in water, ethanol (CH_3CH_2OH), or protein. Therefore, ν depends only on B_L, the local magnetic field around the nucleus. This principle is essential to understanding NMR imaging and spectroscopy because accurate measurement of local magnetic fields in tissues and in molecules provides the spatial and chemical information. This measurement is made by determining the resonance frequency, ν of the nucleus. Another term for resonance frequency is Larmor frequency.

From this point on, we will consider only the average behavior of all of the nuclei of interest. Under equilibrium conditions, the nuclei of a spin $\frac{1}{2}$ nucleus like ^1H or ^{31}P are oriented with or against the imposed field. A small excess of nuclei are oriented with the field because this is the lower energy state. The average alignment of all of the nuclei may be represented by a single magnetization vector, M.

The Radiofrequency Field

If we add another magnetic field perpendicular to the main field, then the average orientation of the nuclei shifts away from alignment parallel to the z axis. This small magnetic field (B_1) may be applied exactly at the precession frequency which efficiently tilts the average magnetization away from the z axis. This event is the resonance phenomenon. Since the B_1 field oscillates at precisely the resonance frequency of the nucleus of interest it is possible to shift the orientation of only those nuclei. Furthermore, the extent of this shift is dependent on the duration of the applied pulse. Generally, the duration of a pulse of r.f. power may be described by the extent to which the average orientation of the nuclei is shifted. A 90° pulse means that all magnetization is rotated away from the z axis and into the x-y plane. A 180° pulse means that the average orientation is parallel with the z axis but oriented in the opposite direction compared to baseline conditions.

Figure 2. Nuclear magnetic resonance. (Opposite page). In a magnetic field, the average orientation of a nucleus is parallel to the applied field (a). After a 90° r.f. pulse, the magnetization is flipped into the x-y plane where it is detected (b). As time passes, the spin gradually loses the net magnetization in the x-y plane. Simultaneously the average magnetization along the z axis increases (c,d,e). Finally, the magnetization returns to baseline (f). This diagram shows a simplified picture of the NMR observation because precession of the nuclei has been omitted.

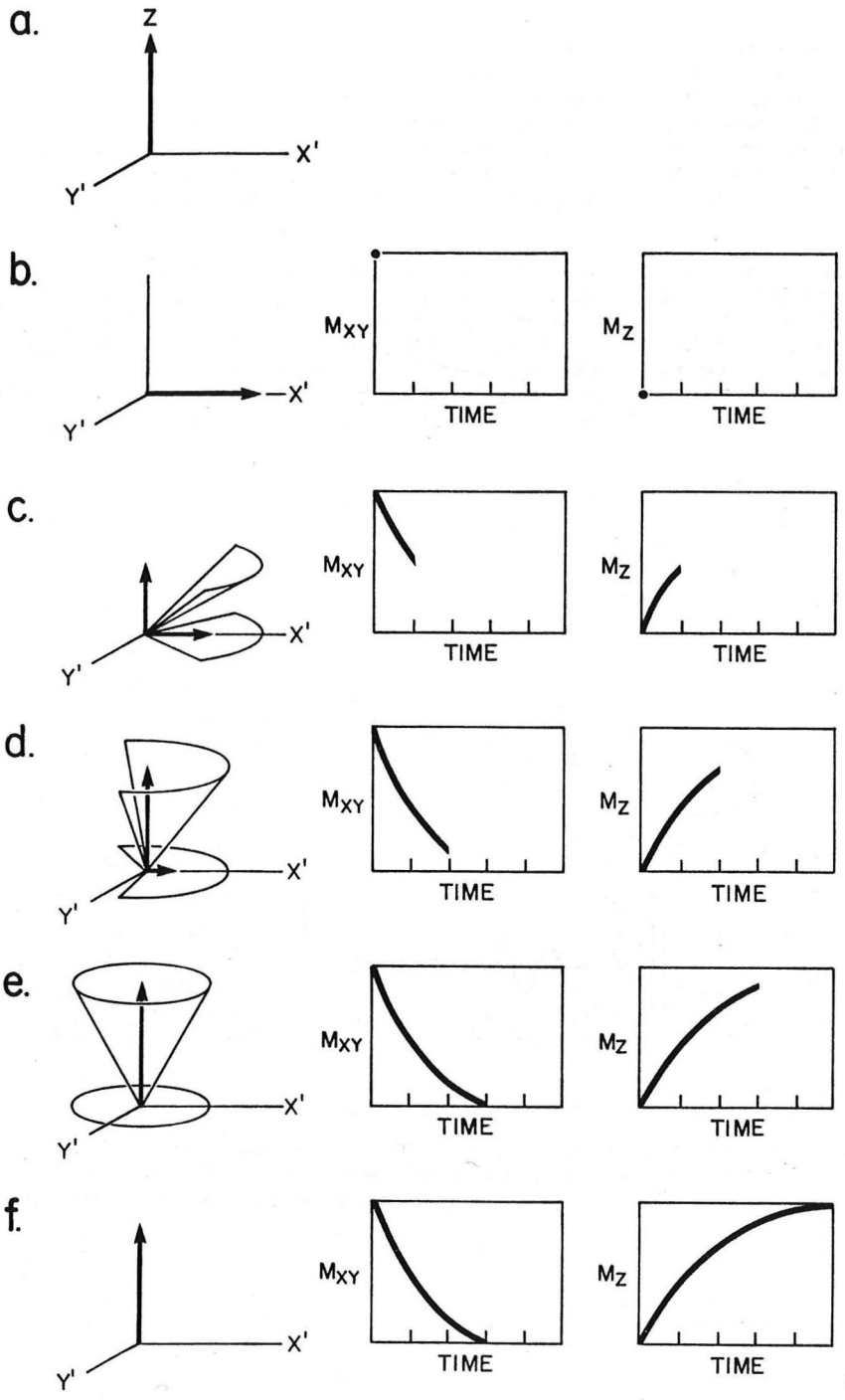
a.
Z
X'
Y'
b.
X'
Y'
M_{XY}
TIME
M_Z
TIME
c.
X'
Y'
M_{XY}
TIME
M_Z
TIME
d.
X'
Y'
M_{XY}
TIME
M_Z
TIME
e.
X'
Y'
M_{XY}
TIME
M_Z
TIME
f.
X'
Y'
M_{XY}
TIME
M_Z
TIME

Detecting Resonance and Signal Processing

Observation of the nuclear spin is made after the r.f. is turned off, as summarized in Figures 2 and 3. The magnetization M will immediately begin to return to its baseline state parallel to the applied field (the z axis). As this average magnetization returns to the baseline state, it precesses around the z axis. This motion of a magnetic dipole induces a voltage in the receiver coil. The voltage alternates at the frequency of precession, and the voltage decays over a period of time. The only magnetization that can be detected is the component of M in the x-y plane, M_{xy}. Therefore, the decay of the signal means loss of M_{xy}.

The signal is detected by a tuned antenna, amplified, and converted to a digital signal for storage in a computer (83). The free induction decay refers to the induction of a voltage in the coil by the nuclear magnetization; free refers to the absence of an r.f. field, i.e., the magnetization precesses freely. This set of data, voltage amplitude as a function of time, may be converted to another representation of the same data, signal intensity as a function of frequency. This conversion, known as the Fourier transform, is generally necessary for analysis of spectroscopic data (50).

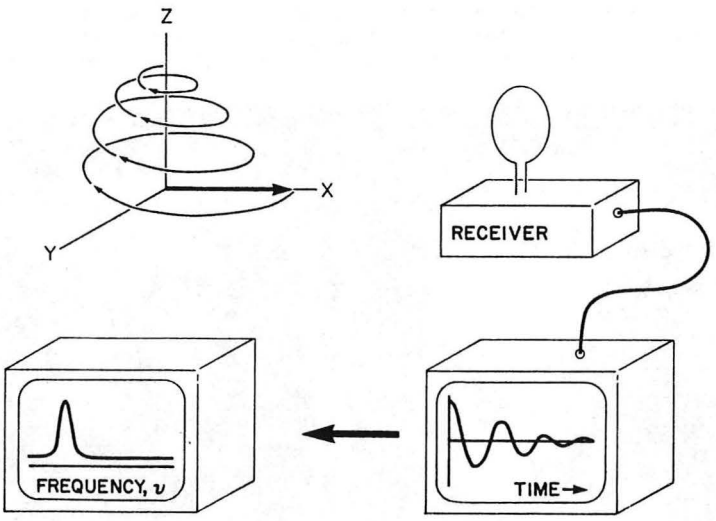

Figure 3. Detection of the signal. After a 90° pulse, the nuclei precess as they return to the equilibrium state. This "motion" of the nuclei is detected by a tuned antenna and stored in a computer where it is subsequently processed.

Relaxation

Once the average orientation of M has been disturbed by the r.f. pulse, several processes combine to return M to its orientation parallel to Z. The effects of these processes are summarized in the measured values, T_1 and T_2. These relaxation times simply describe the rate at which a group of nuclei return to baseline state. The study of nuclear relaxation is an attempt to establish the mechanisms by which a population of nuclei comes into equilibrium with its environment. An appreciation of the processes that these numbers represent is important for two reasons.

First, contrast between tissues in NMR images is strongly influenced by the relaxation times of these tissues. The difference in relaxation times may be exploited to enhance contrast that is not dependent on tissue density. A concept of similar significance is the principle that contrast between tissues on CT scan is due to different x-ray attenuation by those tissues.

Relaxation processes are also important because measurement of T_1 and T_2 may prove clinically useful. A recent case record in the New England Journal of Medicine (March 14, 1985) described a woman with a pancreatic mass. The NMR study "disclosed prolongation of T_1 and T_2 relaxation times." Although this information was not useful in this patient's situation, it was reported presumably because there is some evidence that measurement of absolute T_1 and T_2 may eventually provide diagnostic information. However, the clinical value of measuring T_1 and T_2 is not known. Abnormal relaxation times may prove to be relatively nonspecific indicators of disease.

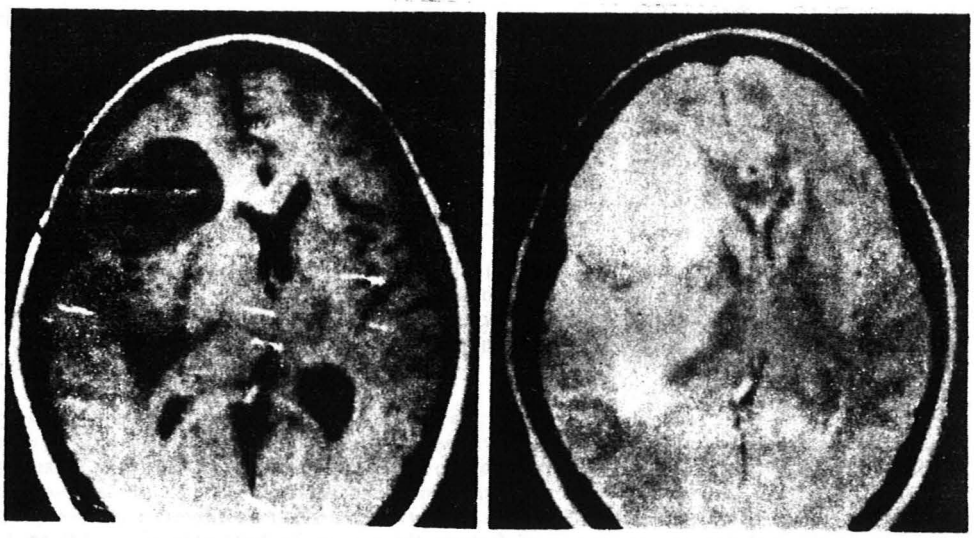

Figure 4. NMR images of a glioblastoma. These NMR images clearly demonstrate the cystic structure in the frontal lobe. On the right the cystic tumor is not differentiated well from the posterior edema. The contrast between gray and white matter is appreciable. On the left the contrast between the fluid-filled cystic tumor and posterior edema is dramatically enhanced. These effects are due to differences in relaxation times of the different tissues. On the left TR/TE is 0.5/28; on the right it is 1.5/56.

To illustrate the importance of relaxation times, the images in Figure 4 were obtained under slightly different acquisition parameters. By simply changing the imaging condition slightly, the relative intensities of the intracraninal tissues have shifted dramatically. This means that the differences in signal intensity between tissues are not due simply to differences in ^1H concentration. The ability of the radiologist to selectively highlight certain tissues depends solely upon the differences in relaxation times of those tissues.

To obtain insight into the events described by T_1 and T_2 we need to consider what happens to the population of nuclei after the magnetization of interest, M, has been rotated into the x-y plane. The events are summarized in Figure 2. The spins generate a signal in the antenna during return of M to the baseline state, and T_1 and T_2 characterize this return. The rate at which magnetization reappears along the z axis is:

$$M_z = M_o (1 - e^{-t/T_1}) \qquad [2]$$

where M_o is the equilibrium magnetization, t is the time after the r.f. pulse is turned off, and T_1 is the spin lattice or longitudinal relaxation time. M_z is the longitudinal magnetization, or the magnetization parallel to z (the component of M parallel to the applied field). This relaxation time characterizes the rate at which the longitudinal magnetization grows after the r.f. is turned off. This relaxation process is sometimes called the spin-lattice relaxation because it involves the exchange of energy between the nuclear spin and the surrounding molecular framework, or lattice. After a 90° pulse, all of the magnetization is in the x-y plane, and M_z is 0. As time passes, M_z grows toward the baseline condition, $M_z = M_o$.

The rate at which magnetization disappears from the x-y plane is characterized by T_2. Two processes contribute to the observed T_2. Spin-spin relaxation involves the exchange of energy between nuclear spin and neighboring nuclear spins. In addition, the nuclear spins that make up M do not precess at exactly the same rate because of local field inhomogeneities. Consequently, they begin to dephase or to spread out in the x-y plane. These combined events are detected as a loss of signal in the x-y plane:

$$M_{xy} = M_o e^{-t/T_2} \qquad [3]$$

assuming that all of the equilibrium magnetization was initially rotated into the x-y plane. M_{xy} is the transverse magnetization, M_o is the equilibrium magnetization, and T_2 is the spin-spin or transverse relaxation time. One simple conclusion from this formulation is that $T_2 \leq T_1$, which may be derived from the relationship $M_{xy} + M_z \leq M_o$.

To a first approximation, then, there are two parameters that characterize the rate at which the spin system comes into equilibrium with the environment. The actual values of T_1 and T_2 in tissues reflect certain aspects of the physical environment of the nucleus in tissue. Relaxation is mediated by the fluctuating magnetic fields in the microenvironment around an observed nucleus. This fluctuating field occurs because all of the molecules (and therefore all nuclei) in a sample are moving due to thermal energy. Some of these relative movements occur at a rate near the Larmor frequency of the observed nucleus. Since these moving nuclei possess a magnetic movement, they generate very small magnetic fields that may fluctuate. In essence, M returns to the baseline state because it interacts with small magnetic fields that are fluctuating relative to M at the resonance frequency. Components of this relative motion along the x, y, and z axis may contribute to T_2. Components along the x and y axis (but not z) contribute to T_1 (52).

The measurement of these relaxation times is not difficult in simple systems. A 180° pulse rotates the magnetization to a new orientation parallel to the z axis, but in the opposite direction. If we wait a period t and then apply a 90° pulse then the magnetization in the x-y plane is related to the rate at which the M_z was returning to the baseline state. This process may be repeated at multiple values of t and an exponential curve obtained. The measurement of T_2 is slightly more difficult to visualize and is discussed in more detail in the section on imaging.

So that is what NMR is all about. Ray Freeman suggested that the nucleus of an atom may be considered a spy residing within a molecule. To discover the "local condition" we can ask certain questions of our many spies in the field. One question is "What is the precise B_L?" The answer is provided by the resonance frequency. Another question, "How many of you are there?" is answered by the signal amplitude. Finally, we could ask "How rapidly do the local conditions change, and in what direction?" The answer is the T_1 and T_2.

2.2 A Complementary Description

The foregoing is a description of NMR in terms of classical physics. Essentially, we assumed that a nucleus with a magnetic moment (spin $\neq$ 0) is adequately modeled by a charged sphere spinning on its axis. This model permits visualization of the behavior of the nucleus during an experiment, and the approach is surprisingly powerful at all levels of NMR theory. However, the classical formulation does not adequately characterize two fundamental aspects of the behavior of a nucleus in a magnetic field: 1) the limited number of orientations available to a magnetic nucleus in a magnetic field, and 2) the distribution of nuclei among these orientations.

Energy Levels of the Nucleus

Certain atomic nuclei possess spin. More precisely, the spin quantum number I determines the number of energy states that are available to a nucleus with spin in a magnetic field. The number of allowed energy states is 2I + 1. Thus, for a nucleus of spin $\frac{1}{2}$ like ^{1}H or ^{31}P there are only two energy states permitted for each nucleus. The difference between these energy states is:

$$\Delta E = \gamma h B_L \qquad [4]$$

where B_L is the magnetic field, h is Planck's constant, and γ is the magnetogyric ratio. For a nucleus to pass from one energy state to the other, it must give up or absorb energy ΔE with frequency ν

$$\Delta E = h \nu \qquad [5]$$

Equations 4 and 5 may be combined to derive equation 1.

$$\nu = \gamma B_L \qquad [1]$$

This is the fundamental relationship describing all NMR observations. Note that terms related to quantum physics (e.g., Planck's constant and I) have dropped out.

Distribution of Nuclei Among Energy Levels

For a nucleus of spin $\frac{1}{2}$ in a magnetic field, the entire population of nuclei (at thermal equilibrium) exist in two orientations, parallel (low energy) or antiparallel (high energy)

with respect to the local field. The number of nuclei in the low energy state exceeds the number (N) in the higher energy state:

$$\frac{N\ low}{N\ high} = e^{\gamma hB_L/kT} \quad [6]$$

where h and K are physical constants (Planck's and Boltzman's, respectively), T is the absolute temperature, B_o is the magnetic field, and γ is the magnetogyric ratio for that nucleus. For medically relevant (temperature = 37° C) samples, this equation may be reduced to:

$$\frac{N\ low}{N\ high} = e^{1.54 \times 10^{-7} \times B_o \times \gamma} \quad [7]$$

where γ is in MHz/T and B_o is in T. Under conditions used for imaging (T = 0.35) at UTHSCD, the ratio of low energy/high energy protons is 1.000002.

This formulation of the NMR experiment relies on concepts from quantum physics and statistical mechanics. Two very important conclusions rely upon this formulation. First, the difference in the number of nuclei in the low or high energy state is dependent on the magnetic field. In a more intense field, the population difference will be increased. Since the sensitivity of the NMR experiment is related to this population difference, NMR observations are more sensitive at higher fields (82).

Second, compared to the energy imparted by the temperature of the sample (37° C), the addition of energy by magnetic fields is trivial. This concept will be developed further in the consideration of safety.

3. A BRIEF HISTORY OF NMR IMAGING AND MEDICAL NMR SPECTROSCOPY

This brief review of the principles of NMR provides the necessary background to appreciate the history of this field. The development of NMR spectroscopy, like most other technical and scientific advances, occurred in the setting of active research in related areas by several groups. In the 1920s and 30s experiments that demonstrated nuclear spin were performed, and the concept of nuclear magnetic resonance was established. Bloch, Hansen, and Packard at Stanford and Purcell, Torrey, and Pound at Harvard were the first to observe NMR in ordinary materials. Proton magnetic resonance was detected in parafin and in water, and the observations were reported in consecutive issues of the Physical Review in 1946. Initially, Bloch's group termed their observations "nuclear induction" and Purcell's group "nuclear magnetic resonance". At the time of their discovery, it was not appreciated that both groups had observed the same phenomenon. This brief delay was due to the different but complementary mathematical formulations by each group. This question was resolved quickly because the observations attracted immediate interest. Felix Bloch and Edward Pucell were awarded the Nobel Prize in Chemistry in 1952 (14,130).

Initially, it was thought that NMR could provide a very precise method of measuring the gyromagnetic ratio of the nucleus, γ. It was soon discovered that the measured γ actually depended upon the compound in which that nuclear resided. One of the earliest NMR spectra ever obtained was that of ethanol. This spectrum showed that there are three types of ^1H in CH_3CH_2OH, and they are present in a 3:2:1 ratio. The difference in resonance frequency of nuclei in different chemical sites was called the chemical shift. Organic chemists found this effect very useful for structure elucidation, and NMR spectroscopy was born. According to Martin Packard, "The organic chemists got the point very quickly, thanked the physicists, and took over."

Over the next 20 years, there was a tremendous expansion of interest in NMR applications. It became a major analytical and research tool. The method was widely applied by organic chemists, inorganic chemists, and biochemists for studies of chemical structure and kinetics. In 1973, 27 years after the descriptions by Bloch and Purcell, two more landmark papers were published. Paul Lauterbur published the first NMR images of a pair of water-filled capillary tubes. He emphasized that in a field gradient the resonance frequency of each nucleus is determined by its position in the field. He also showed that T_1 of the solution dramatically influenced images, and he described T_1 "weighted" images (98).

Also in 1973, Moon and Richards showed that phosphorus spectra could be obtained in blood and that intracellular pH could be measured non-invasively by NMR (117). In 1974, David Hoult and the group at Oxford demonstrated that similar observations could be made in skeletal muscle (81).

Since these observations, both NMR spectroscopy and imaging have developed dramatically. At the time Lauterbur published the first images, other groups were pursuing related avenues of research. Damadian in 1971 reported that in biopsy specimens of neoplastic tissue the proton T_1s were different from normal tissue (36). In 1972 he filed a patent that proposed without detail that the human body could be scanned for clinical purposes (4,5). Mansfield in 1973 was developing NMR for imaging (107). In the latter half of the 1970's several papers appeared describing new NMR imaging techniques that were significantly different from Lauterbur's original proposal. In 1976, the first image of a human finger was reported, followed quickly by images of the hand and thorax in 1977 and the head and abdomen in 1978 (41,42,73,105,106). It is remarkable that only ten years after Lauterbur's paper a book was published containing clinical results with NMR imaging from seven centers (126).

4. CLINICAL NMR IMAGING

The fundamental principle of NMR imaging is that the position of a nucleus is determined by measuring its resonance frequency. This principle may be illustrated on a large scale. Assume that you have a radio receiver that detects radiowaves between 99 and 100 MHz. Assume also that we place a radiotransmitter somewhere along the line between the Fort Worth Stockyards and Reunion Arena in Dallas. This radiotransmitter changes its frequency between 99 MHz in Fort Worth and 100 MHz in Dallas as a linear function of its position between the two cities. For every mile it comes closer to Dallas, it adds 0.031 MHz to the transmitting frequency. By tuning the receiver in Dallas, we can measure the frequency at which the radio is transmitting. For example, if we find the signal at 99.47 MHz, we would know that the transmitter is somewhere in Arlington. Thus, we obtained very good spatial information without using anything more complicated than a radio receiver similar to the one in your car. All we needed was a very precise radiotransmitter that changed its frequency depending on its position.

4.1 Principles of Image Formation by NMR

Recall that we found that $\nu = \gamma B_L$, that is, the Larmor frequency of a nucleus provides very precise information about the intensity of a local magnetic field. If we apply a magnetic field gradient that is linearly proportional to distance, then the location of a sample within that field can be determined by its resonance frequency as shown by Figure 5. This principle has long been recognized (58). If the magnetic field varies over a sample, then a particular nuclear species no longer resonates at a fixed frequency. This principle may be employed to obtain spatial information, as

Lauterbur demonstrated, in more than one dimension. For example, along the x axis of the sample the field is held constant. Along the y axis the field varies as a linear function of distance. At every frequency the amplitude of the signal reflects the total number of atoms along that line parallel to the x axis. This single "projection" does not provide sufficient information to reconstruct the image. However, if the magnetic field gradient is rotated, a different projection of the sample is produced. This is exactly the approach taken by Lauterbur. Once multiple projections have been obtained, it is possible to reconstruct the original image by the projection-reconstruction method identical to the process used for x-ray computed tomography (21).

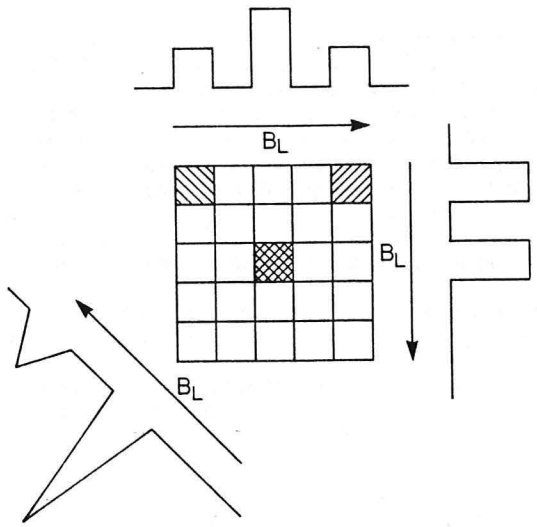

Figure 5. NMR imaging by projection reconstruction. Three objects are imaged in this sample. The concentration of the detected nuclei is twice as great in the center as at the corners. Along each arrow is a small gradient in the field experienced by each nucleus.

Imaging Techniques

Since Lauterbur's description, several distinct methods for generating an NMR image have been developed and demonstrated. The techniques vary significantly in their efficiency, speed, flexibility, technical difficulty and computational demands (32-35,38,-46,64,84,86,95,124,131). A review of all imaging techniques and their variants is far beyond the scope of this review. Suffice it to remark that one efficient approach is the two-dimensional Fourier transform method with near-simultaneous acquisition of multiple slices. Reviews of the various imaging methods are available (85,107).

Pulse Sequences

Regardless of the specific imaging technique, certain r.f. pulse sequences have become standard. The spin echo and inversion recovery sequences are available on all of the NMR imagers approved by the U. S. Food and Drug Administration. Other sequences are available from some manufacturers.

In its simplest form the spin echo sequence consists of a 90° pulse followed shortly by a 180° pulse. The 90° pulse rotates the magnetization into the x-y plane. After the r.f. is turned off recovery of magnetization begins. M_{xy} decays because of the two processes described previously: spin-spin relaxation and local magnetic field inhomogeneities. Dephasing reduces detectable signal. However, the loss of M_{xy} due to local field inhomogeneity can be reversed by application of a 180° pulse as shown in Figure 6. Magnetization detected at this time is the spin echo, and in the actual data used to generate an image.

The following abbreviations are used to describe the timing of pulse sequences:

TR: Time to repetition of pulse sequences. This is the time between the beginning of each pulse sequence.

TE: Time to acquisition of echo. This is the time between the 90° pulse and the peak echo formed by the 180° pulse.

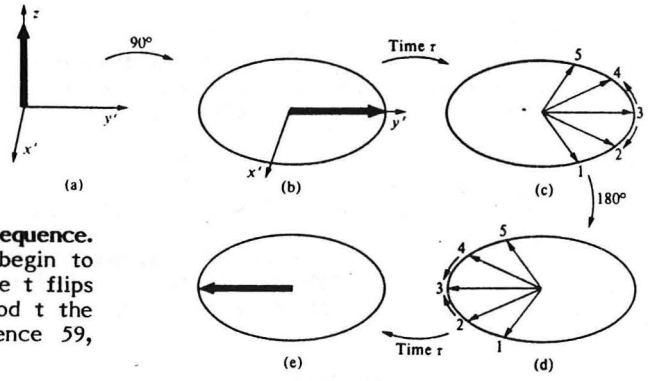

Figure 6. The spin echo pulse sequence. After a 90° pulse (b), the spins begin to dephase (c). A 180° pulse at time t flips the spins (d). After another period t the spins have rephased (from reference 59, page 120).

Both TR and TE are to some extent under operator control. Changing TR and TE may dramatically alter image contrast, as may be appreciated in Figures 4 and 7. Recall that after a 90° pulse there is no magnetization along z. This magnetization must be allowed to recover before repeating the pulse sequence. If the protons in a tissue have a short T_1, more recovery will have occurred for a given delay than for protons with a long T_1. Consequently, if TR is long (2.0 sec) then protons in both tissues return to their baseline condition between pulses. However, if TR is short (0.5 sec) then the protons than in different tissues will not recover to the same degree. Thus, a spin echo sequence with a short TR will tend to enhance the difference in T_1 between tissues. Conversely, a long TR will allow all protons to recover and T_1 dependent contrast will vanish. After the 90°-t-180° sequence the echo is received or "read" at 2t. If the delay t between the 90° and 180° pulse is short, very little transverse relaxation will have occurred. With longer delays those protons with a long T_2 will produce more signal than those protons with a short T_2. Thus, a long TE tends to enhance T_2 dependent contrast. If TR is long then all protons (regardless of T_1) will have recovered to their equilibrium magnetization prior to the next pulse, thereby losing T_1 information. If TE is short, none of the protons will have relaxed significantly (regardless of T_2), thereby losing T_2 information. This combination of long TR and short TE tends to produce proton density-dependent contrast. These relationships are summarized in Table 2.

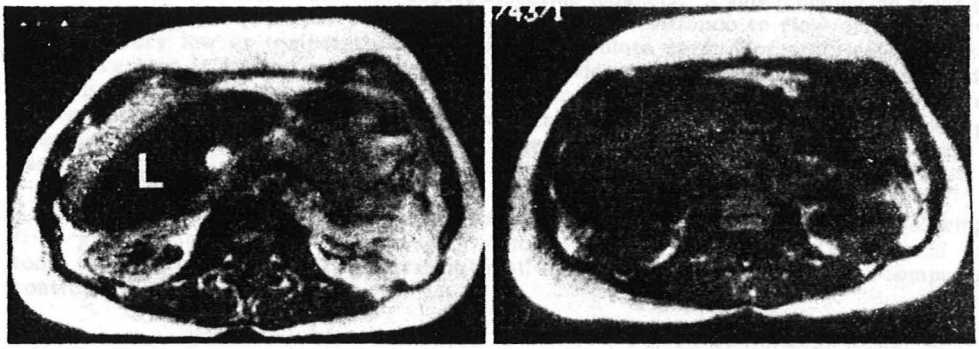

Figure 7. NMR images of a patient with ascites. On the left the TR is 2.0 sec and TE is 28. On the right, the TR is 0.5 sec and TE is 28. The reversal of contrast between liver and ascites in the right image is due to the long T_1 of ascites fluid.

TABLE 2

INFLUENCE OF TR AND TE ON IMAGE CONTRAST USING THE SPIN-ECHO TECHNIQUE. TE AND TR ARE PARAMETERS UNDER OPERATOR CONTROL

TR	TE	Contrast Between Tissue is Enhanced By
Long	Short	^1H density difference
Short	Short	T_1 difference
Long	Long	T_2 difference

4.2 The Imaging System

As we have seen, the four essential components of any NMR experiment are the sample, the magnetic field, the r.f. field, and the detecting system. Certain features of each component should be emphasized as they apply to NMR imaging (Figure 8).

Sample

The sample is a human. More precisely, the sample is that portion of a person within the transmitter and receiver coils of the spectrometer. The nucleus to be detected in clinical imaging is ^{1}H which is present in the human body predominantly as water.

Magnet

Imaging has been performed with three types of magnets: permanent magnets, resistive magnets, and superconducting magnets. Each type is available commercially. Permanent magnets for imaging are simply larger versions of the magnets of everyday experience. Resistive magnets are those in which a magnetic field is generated by passing current through multiple turns of copper wire. These magnets have the disadvantage of requiring cooling water and substantial electrical power; however, they are light and less difficult to construct than superconducting magnets. A superconducting magnet takes advantage of a property of certain alloys: the resistance to flow of electricity becomes very low at temperatures approaching absolute zero. For practical purposes once a current is started no energy needs to be added to maintain the magnetic field. The disadvantage of this system is the requirement for maintaining the temperature of the magnet wire near absolute zero, which requires very special insulation and cooling agents. Nevertheless, this is the type of magnet in general use by commercial manufacturers.

A special aspect of the magnetic field for imaging is the requirement for generating field gradients. Therefore, all imaging systems possess extra coils (maintained at room temperature) for rapidly generating small magnetic field gradients under computer control.

Figure 8. Schematic drawing of a superconducting NMR imaging magnet and coils

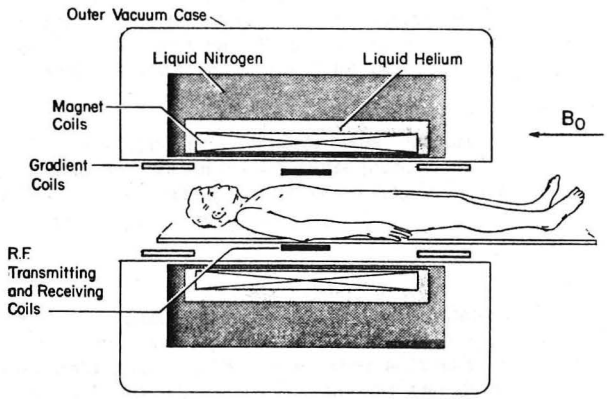

Radiofrequency Magnetic Field

The radiofrequency magnetic field is provided by standard coils under computer control. The frequency at which the system operates is determined by the field, according to the relationship in Equation [1]. For certain requirements peculiar to imaging (slice selection) the r.f. pulse must be shaped to limit the region excited by it.

Detecting System

The receiver coil may encircle the body or it may be a surface coil (see Section 5.2). Detection and analogue-to-digital conversion yields data which is stored in computer memory. The imaging sequence may be repeated to increase the signal-to-noise ratio of the final image. Results of repeated sequences are summed in memory and then transformed into an image by mathematical techniques that in essence reverse the imaging process.

4.3 Interpretation of NMR Images: Contrast and Tissue Characterization

The typical NMR image is a thin-slice tomographic section obtained in the coronal, sagittal, or transverse planes of the human body. Each picture element (pixel) is about 1.5 X 1.5 mm, and represents a slice about 5 mm thick. Thus, each pixel represents a 1.5 X 1.5 X 5 mm volume element (voxel). The techniques described in the previous section make it possible to translate the spatial distribution of ^1H nuclei in the sample to an ^1H image. The intensity of each individual pixel in the image reflects multiple aspects of the protons in the volume element that each pixel represents. The relevant parameters are specifically the concentration of hydrogen nuclei, $N(^1H)$; the motion or flow $f(^1H)$; and the T_1 and T_2 of hydrogen nuclei in that volume. For example, in a spin echo sequence the signal intensity from a volume element is approximately (125):

$$\text{Intensity} = N(^1H)\, f(^1H)\, (e^{-TE/T_2})\, (1 - e^{-TR/T_1}) \qquad [8]$$

For an inversion-recovery technique the formulation is slightly more complex because of a dependence on TI. In general, it is useful to consider pixel intensity as the result of a complex function of imaging parameters and tissue relaxation times. TR, TE, and TI are to some extent under operator control. Within certain limits imaging parameters may be selected to enhance contrast between tissues with different T_1 or T_2. Note that intensity also depends on flow or motion. This has the effect of reducing signal from the lumen of vessels, and suggests that flow may be measured (18,65,144,145).

Accurate interpretation of an NMR image depends upon two factors. Most important is a knowledge of the usual features of a disease and its anatomic consequences. This information is, of course, independent of NMR. The other factor is an appreciation of the factors that influence tissue ^1H relaxation times.

Water and Lipid in Tissue

The composition of normal tissue may for our purposes be reduced to two chemical structures: water (H_2O) and lipid ($-CH_2-$). The vast majority of protons in tissue reside in these compounds. Body fat is about 60% lipid and 10-20% H_2O; other soft tissues are about 60-70% water with a small fraction of lipids. Compared to muscle and liver, fat has a short T_1 and a long T_2 which is due to its lipid content. Most of the pathologic changes in tissue detected by NMR appear to be due to changes in H_2O content and state of the tissue. Therefore, intracellular H_2O will be considered in more detail.

The state of water in tissues influences the results of clinical NMR imaging. The state of water refers to the many factors which alter the observed relaxation times of water protons. For example, binding of H_2O to large proteins or exposure of H_2O dissolved paramagnetic substances (like O_2) may reduce the relaxation time. As shall be seen, these effects are generally not specific for any disease, but are very important for producing contrast between normal and pathologic tissue.

Figure 9. Contrast enhancement in solid tissues. The hemangioma (H) and spleen (S) are very sensitive to changes in pulsing parameters. (TR/TE 0.5/56 in the left and 2.0/56 on the right).

The state of H_2O in the cytosol is the subject of considerable controversy (94,97). According to the traditional model, water in the cytosol is in an aqueous phase, and proteins and electrolytes are in dilute solution. According to this model, the NMR properties of tissue water are similar to any simple aqueous solution. The alternative hypothesis proposes that all water in cells is in a highly ordered or semicrystalline state. Some insight into the behavior of cellular water that is relevant to NMR imaging may be obtained from the traditional model, which is sufficient for our purposes (29,107).

We may assume that water in cells exists in two phases. In the aqueous phase it behaves exactly like any bulk water solution. The T_1 of ^1H in water is about 2.8 seconds. Roughly 90% of tissue water is in this state. The remaining 10% of tissue water is bound to or associated with macromolecules. Consequently, the T_1 of bound water is reduced to about 0.1 second. Because the water is in rapid exchange between these states, a single exponential is recorded if T_1 is measured. This two-state model predicts that

$$T_{1\,obs} = \frac{T_{1b}\,T_{1f}}{(1-f)(T_{1f}-T_{1b}) + T_{1b}} \qquad [9]$$

where f is the fraction of cell water that is not bound to macromolecules, T_{1f} is the T_1 of free water, T_{1b} is T_1 of bound water, and $T_{1\,obs}$ is the observed T_1. If the assumptions cited above are approximately correct (f = 0.9, T_{1f} = 2.8 sec, T_{1b} = 0.1 sec), then the observed T_1 is about 750 msecs, which is in the range of T_1 reported for ^1H in biological systems (0.5-1.5 secs). It should be emphasized that relaxation times can be predicted only for very simple systems. There is no comprehensive and widely accepted formulation that characterizes the relaxation times of tissue H_2O.

Significantly, this formulation predicts that if free water in the tissue increases by a small amount (for example, if f increases from 0.90 to 0.92), the change in T_1 will be proportionately much greater. Effectively, a small change in free water has amplified

effects on T_1, as summarized in Figure 10. The "wetter" the tissue the longer the T_1.

The assumptions incorporated in Equation 9 should be considered a crude and qualitative model of tissue water. Nevertheless, this model predicts that the water content of tissue will significantly influence T_1 and, therefore, image contrast.

The value of absolute T_1 and T_2 measurements of normal or diseased tissue is unknown. Generally, there is little overlap between relaxation time of normal and diseased tissues. Therefore, contrast in NMR images is good. However, there is considerable overlap in relaxation times among pathologic condition. Therefore, it is not likely that NMR imaging will discriminate among different types of pathology based on T_1 and T_2.

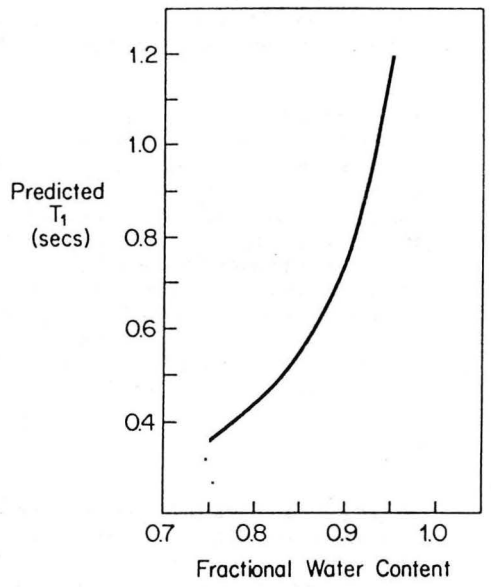

Figure 10. Influence of fractional water content on T_1

Neoplasms

^1H relaxation times are greater in immature skeletal muscle compared to mature skeletal muscle (74). The subsequent observation that relaxation times are greater in neoplastic tissue compared to normal is consistent with the hypothesis that reduction of T_1 is associated with cellular differentiation (36). This phenomenon has been confirmed in laboratory animals as well as in human tissues (10,37,48,75,80,88,101,114,149). The T_1 of tissue ^1H involved by neoplasm is roughly 50% greater than the T_1 of normal tissues. The mechanism of the increase in T_1 is not known, essentially because the factors influencing proton T_1s in any tissue are not completely understood (118). It is clear that water content (and presumably free water) plays a significant role. In one study of normal and neoplastic tissue the fractional water content (ranging from 0.65 to 0.90) predicted the T_1 in seconds remarkably well: $T_1 = 8f - 5$ (93). The changes in T_1 are probably not due simply to irreversible changes in water content since T_1 varies cyclically in synchronized populations of HELA cells without significant change in H_2O content (9).

These data should be interpreted with three cautions in mind. First, almost all of the published work on T_1 of neoplastic tissue comes from work in vitro. There is little quantitative information about relaxation times in vivo. Second, much of the literature reports experiments with rapidly proliferating tumors in animals. The excellent discrimination between normal and malignant tissues in animals may not be confirmed in humans because the tumors grow more slowly. Finally, one group has observed changes in T_1 in tissues distant to a neoplasm, suggesting that a systemic effect of a malignancy could obscure the diagnosis (if it is dependent on T_1) of metastasis.

Tissue Infarction

Another area of intense research interest is ^1H NMR imaging of tissue infarction. The results are similar for brain, skeletal muscle, and heart: T_1 and T_2 are increased compared to control. Several groups have found that relaxation times are prolonged in acutely ischemic or infarcted myocardial tissue (55,78,89,115,136,153-155). Associated with this increase in T_1 is an increase in tissue water, as predicted by Equation [8]. Water content and T_1 of reperfused myocardium is also greater than normal myocardium.

The precise relationships among tissue water, T_1, reduced blood flow and reperfusion are not known. Early in ischemia several groups have reported increases in tissue water, although this finding is not universal. All groups, however, report an increase in T_1. With reperfusion there is a dramatic increase in tissue water (predominantly intracellular fluid), at least during reflow after 40 minutes of ischemia. This observation is interesting because there is little further change in T_1 with reperfusion. This implies that the mechanism of the increase in T_1 is not due simply to an increase of free water. Rather, there may be a significant change in the state of water that is not modeled by the two-phase relationship. Further compounding the complexity of this issue is the observation by Michael, et al. that H_2O content and relaxation times in cardiac mitochondria are reduced early in ischemia. Thus, water in at least three distinct compartments (mitocondria, cytosol, and extracellular space) may contribute to the observed T_1.

Contrast Agents

These agents do not, in fact, produce contrast in the sense that barium or angiographic dye produces contrast. In NMR images the contrast agents are actually relaxation enhancing agents. They are not imaged directly. Certain compounds in very small concentration significantly alter the relaxation times of tissue water protons (19,20,26,-66,152). For example, one of the lauthanides, gadolinium, in organic complexes very efficiently reduces the T_1 of water protons in concentration far below toxic. Therefore, there is considerable interest in developing agents that localize specifically (monoclonal antibodies binding to tissue antigens) or nonspecifically (regions of edema). Since image contrast is dependent on relaxation time, it is likely that these agents will play an important role in improving the specificity of NMR diagnosis.

5. CLINICAL NMR SPECTROSCOPY

Certain phosphate-containing metabolites are present in sufficiently high concentrations to be detected by NMR in human tissue. Typically, ATP, phosphocreatine, inorganic phosphate, and phosphomonoesters are detected, depending on the organ. Because these compounds are metabolically relevant, the vast majority of NMR spectroscopy of patients and normal volunteers has been of phosphorus. For this reason, we will review in some detail the principles necessary to interpret a phosphorus spectrum. With modification these principles also apply to spectroscopy of other nuclei (3).

5.1 Information available in a high-resolution spectrum.

Recall that $\nu = \gamma B_L$. Let us assume that the applied magnetic field B_o is constant throughout the sample. If the sample is a liver, and if we are detecting ^1H, then a single resonance is detected which is due to the protons in water which are present in very high concentration. However, if we detect phosphorus, we see a much different spectrum. Multiple peaks are present even though the applied field is homogeneous.

This occurs because there are several populations of phosphates that experience slightly different magnetic fields. These slight differences in local fields occur because nuclei do not exist as isolated entities. The neighboring electrons are negatively charged particles that are in motion. Because they are moving, they constitute a small current and, therefore, generate a small magnetic field. The field generated by the electron is very sensitive to molecular structure which is reflected in the field experienced by the nucleus and, therefore, the resonance frequency.

The average magnetic field acting on a nucleus in a molecule is usually slightly less than the applied field. This occurs because molecular electrons in the presence of an applied field develop currents that tend to oppose the applied field.

To a small degree the nucleus is shielded from the applied field B_o. This shielding (and B_L) is very sensitive to molecular structure. The local field is reported as frequency of resonance according to Equation [1]. A high-resolution spectrum is a plot of the intensity of energy release as a function of the frequency of energy release. Frequency is directly related to the shielding. As described previously, the frequency of a peak is characteristic of the nucleus.

The term "high resolution" is sometimes applied to this type of spectroscopy. This simply refers to distinguishing resonances that differ in frequency by a fraction of a part per million. This very precise measurement of frequency in NMR spectroscopy provides the chemical information described above.

Identification of a Compound

The precise distribution of electrons around a nucleus is determined by multiple factors. A dominant factor is the structure of the molecule. The example shown in Figure 11 demonstrates that the phosphocreatine resonance may be easily distinguished from the three phosphates of ATP. Furthermore, the phosphorus spectrum identifies each phosphorus nucleus and allows us to distinguish different atoms in the molecule. Certain compounds like ATP have characteristic chemical shifts that cannot be confused with any compound except another nucleoside triphosphate. Other compounds such as the sugar phosphates have chemical shifts that are similar and, therefore, cannot be identified specifically in a phosphorus spectrum. We simply can identify the presence of a phosphomonoester.

Relative Concentration

The relative concentrations of compounds present in a spectrum may be determined by integrating the peak areas of the compounds of interest. This approach assumes that the spectrum is accumulated under conditions that do not partially saturate a nucleus. Although suggestions for measurement of absolute concentration have been made, generally the results of any in vivo NMR are reported in terms of relative concentration.

pH Measurement

Another example of the effect of chemical structure on chemical shift is the influence of pH on the resonance frequency of the phosphorus nucleus of inorganic phosphate. This observed chemical shift is related to pH of the solution by

$$pH = 6.75 + \log \left(\frac{\sigma - 3.27}{5.69 - \sigma}\right) \qquad [10]$$

where σ is the chemical shift difference in ppm between the phosphocreatine and inorganic phosphate signal (63). The ability to measure intracellular pH nondestructively is of interest because the $[H^+]$ plays a substantial role in regulation of enzyme activity and cell differentiation as well as reflecting the metabolic state of the cell.

Free Mg^{++}

Mg^{++} alters the chemical shift of the ATP phosphates. The ATP α phosphate is least sensitive to this effect and the ATP β phosphate is most sensitive to the concentration of Mg^{++}. The concentration of free Mg^{++} in the cytosol may be measured by measuring the chemical shift difference between the ATP α phosphate and the ATP β phosphate. This approach assumes that ATP does not bind any other divalent cations in concentrations approaching Mg^{++} (69).

Relaxation Times

The T_1 and T_2 of ATP phosphates may be measured in tissues. It is interesting that in the liver the T_1 of ATP phosphates is about 0.2 secs. In all other tissues studied, the T_1 is 1-2 seconds. This observation indicates that the physical environment of ATP in the liver is significantly different than that in other tissues.

Reaction Kinetics

It is possible to directly measure flux through certain enzyme catalyzed reaction in perfused tissue by NMR. The most widely-studied system in cardiac and skeletal muscle is the creatine kinase reaction. In principle, these measurements may be obtained in vivo (104,123,143).

5.2 Spatial Localization

The usual NMR spectroscopy experiment does not provide spatially localized spectra. This means that simply obtaining a ^{31}P NMR spectrum of the chest, for example, would not be useful because the relative contribution of the heart and skeletal muscle would not be known. The spectrum of the tissue of interest must be resolved from the spectrum due to the surrounding tissue.

One approach to the problem of spatial localization is the suface coil (1). A surface coil is simply one or two loops of wire tuned to the frequency of interest. It may be positioned adjacent to a tissue to obtain a high-resolution spectrum. This remarkably simple approach has proven successful for the study of skeletal muscle and brain in humans. However, for the heart, liver, and kidney the simple surface coil will not suffice. Three alterantives that would permit noninvasive acquisition of ^{31}P NMR spectra from deep organs have been proposed.

Topical magnetic resonance relies on shaping the B_o field in such a way that the tissue of interest is within a homogeneous magnetic field (67,68). A spectrum may be obtained from this tissue. The steep magnetic field gradients in the surrounding tissue prevent acquisition of a high resolution spectrum (which is dependent on a homogeneous field). Two other independent approaches take advantage of the gradient in the r.f. field produced by a surface coil (see 70,72). To date, there is one description of true ^{31}P NMR imaging in the literature. Imaging times were long and resolution (spatial and chemical) was poor. Nevertheless, this publication represents a significant advance in view of the technical problems that were overcome (110).

5.3 Phosphorus NMR Spectroscopy In Vivo

The only published spectra of human tissues in vivo are brain and skeletal muscle (Figure 11). Human kidneys prior to transplant have also been described. Based on published data in humans and experimental animals a summary of the typical ^{31}P NMR spectrum to be expected from each organ is provided in Table 3 (8,53,67,81,87).

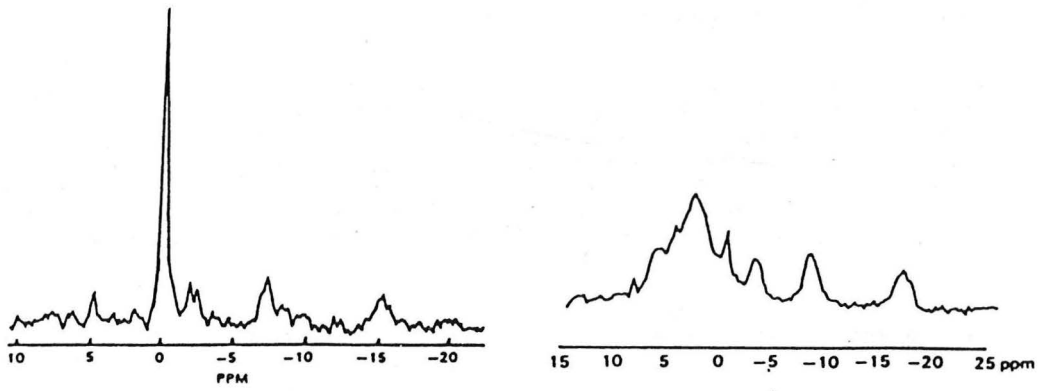

Figure 11. ^{31}P NMR spectra of human tissue. On the left is an example of human skeletal muscle (from 147) and of human brain (133) on the right.

TABLE 3

RELATIVE CONCENTRATION OF PHOSPHATE-CONTAINING COMPOUNDS AND pH DETECTED IN MAMMALIAN TISSUE BY ^{31}P NMR

	Brain	Heart	Skeletal Muscle	Liver	Kidney
ATP	1	1	1	1	1
Phosphocreatine	1	2	5	0	0
Phosphodiester	2	0.1	0	0.5	0.5
Inorganic phosphate	1	0.1	0.1	0.6	1
Phosphomonoester	1	0	0.1	0.5	1
pH	7.1	7.0	7.0	7.2	7.2

Skeletal Muscle

Phosphorus NMR spectroscopy has been most extensively applied to the study of normal muscle physiology in volunteers, and to the investigation of certain disorders of muscle metabolism in patients. These studies are performed at a field of about 1.9 T with a 3/4"-1" diameter surface coil placed over the flexor muscles of the forearm. The patient places the arm in the magnet for study. Multiple ^{31}P NMR spectra may be obtained at rest and during exercise and recovery. Using this rather simple approach it is possible to monitor the relative concentration of detectable metabolites and pH under various conditions of exercise and ischemia. This approach has been adopted by several laboratories. The results from normal volunteers are in reasonable agreement (6,27,28,31,47,147).

These results provide the standard to which observation in patients may be compared. The protocol in Oxford used a 1" diameter surface coil placed over the flexor digitorum superficials. ^{1}H and ^{31}P NMR spectra are recorded at rest, during aerobic exercise, and during recovery. The exercise consists of squeezing a sphygmomanometer bulb to pressure between 120 and 300 mmHg every two seconds for 1 to 20 minutes. Consistently during aerobic exercise acidosis develops, [phosphocreatine] falls, [ATP] is constant, and [inorganic phosphates] rise. Recovery of phosphocreatine, inorganic phosphate and pH may also be monitored as a function of time (147).

Several reports have recently appeared describing abnormalities in muscle metabolism of patients with weakness. To interpret these results, it is necessary to review briefly some basic biochemistry (Figure 12).

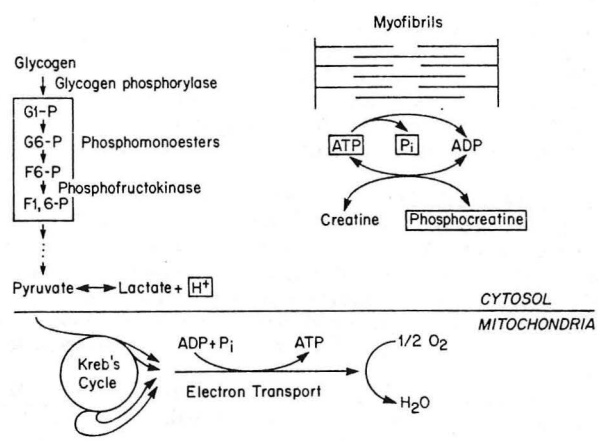

Figure 12. Phosphate metabolism in striated muscle. The compounds in boxes are detected in a ^{31}P NMR spectrum.

TABLE 4

SUMMARY OF THE METABOLIC RESPONSE TO EXERCISE OF THE FOREARM IN PATIENTS WITH SKELETAL MUSCLE DISEASE

The resting ^{31}P NMR spectrum of the forearm muscle was normal in each patient. Details of these studies are available in references 7, 28, 135, and 138.

	pH		[Phosphocreatine]	
Syndrome	Exercise	Recovery	Exercise	Recovery
Post-viral fatigue	Early ↓	Normal	Normal (?)	Delayed
Mitochondrial myopathy	Early ↓	Normal or rapid	Early ↓	Delayed
McArdle syndrome	No Δ	---	Early ↓	Normal
PFK deficiency	No Δ	---	--	---

Disorders of Glycolysis. Patients with the McArdle syndrome complain of the early onset of fatigue, pain, and cramping in skeletal muscle during exercise. Patients with the McArdle symdrome have been studied by NMR in detail. During aerobic and ischemic exercise of the forearm (Figure 1 and Table 4), normal volunteers develop a substantial intracellular acidosis. The NMR observations were substantially different in the patient with McArdle syndrome. There was no change or a slight increase in intracellular pH during exercise that caused a substantial decrease in phosphocreatine and accumulation of inorganic phosphate. These results may be interpreted as follows: during exercise skeletal muscle normally uses glycogen and produces lactate as an end product of glycolysis which is associated with acidosis. In the absence of glycogen phosphorylase, substrate does not enter the glycolytic pathway; consequently, acidosis does not develop.

Patients with deficiency of skeletal muscle phosphofructokinase also report weakness. Patients with PFK deficiency have been studied by NMR during exercise. Both groups report a dramatic increase in the concentration of sugar phosphates in the muscle during exercise, and no change in intracellular pH. These observations are substantially different from normal volunteers, and strongly suggest that glycolysis is impaired (because acidosis does not occur). The block occurs early in the glycolytic sequence because sugar phosphates accumulate (28,47,138).

Mitochondrial Myopathies. Mitochondrial myopathies are uncommon causes of weakness and exercise intolerance. Characteristically, gross abnormalities of muscle mitochondria are evident in electron micrographs. Presumably these patients have abnormalities of ATP generation by oxidative phosphorylation, but glycolysis and regulation of intracellular pH should be normal. Two sisters have been studied with deficiency in mitochondrial NADH coenzyme Q reductase of skeletal muscle. Results are summarized in Table 4. The very slow recovery of phosphocreatine was attributed to delayed regeneration of ATP by oxidative metabolism (135).

Post Viral Fatigue. This patient was reported recently (7). A 30-year-old physician developed chicken pox at age 26. After the acute phase of his illness, he was left with severe fatigue that forced him to stop working. Physical exam were normal, and serum creatine kinase was normal. The skeletal muscle biopsy did not show evidence of inflammation, but type II fibers were dominant. The ^{31}P NMR spectra of arm muscle at rest was normal. The results during exercise and recovery are summarized in Table 4. The authors concluded that early acidosis could be responsible for fatigue, and they speculated that the disorder was due to an abnormally large contribution of glycolytically-derived ATP to the total ATP pool.

Duchenne Muscular Dystrophy. This disease is an inherited (sex-linked recessive) disorder that involves proximal and axial muscles, initially. It is associated with elevated serum creatine kinase levels that are highest in the preclinical phases of the illness. This form of muscular dystrophy is also associated with a cardiomyopathy late in the illness. Patients with this disorder have been studied by NMR spectroscopy by two groups (47,122). Both groups noted a decreased [phosphocreatine]/[ATP] and an increased [Pi]/[ATP].

Brain

^{31}P NMR of the normal adult human brain has been reported in three groups (16,133,150). Characteristically, the human brain spectrum is dominated by a very prominent phosphodiester resonance (Figure 11). Welch et al. have recently reported brain ^{31}P NMR spectra of the brains of stroke patients (150). The phosphodiester resonance was unchanged, but the phosphocreatine and phosphomonoester resonances were decreased. Infants with a history of cerebral anoxia were studied by Cady et al. (25). They found that a history of cerebral anoxia was associated with a decrease in high energy phosphates which partially resolved as the patients improved clinically.

Thus, phosphorus spectra may be obtained from the human brain. These studies suggest that regional and global metabolic disorders of the brain may be monitored by NMR.

6. Safety of Clinical NMR Studies

The safety of the clinical NMR studies that are now routinely available may be considered from two perspectives. The essential effects of an NMR study are those that are inherent to the observation. This category includes the effects of radiowaves, static magnetic fields, and switched field gradients. The accidental consequences of an NMR study are those situations that could arise during a study, although the probability is low.

The literature on effects of exposure of tissue to r.f. and magnetic fields is extensive. There is some disagreement about certain effects of prolonged exposure of humans to electric and magnetic fields (2,11,49,51,56,71,99,100,102,116,119). Nevertheless, authorities agree that under the conditions currently used for NMR imaging there is no known hazard (22,30,43,108,120,139,148).

6.1 Effects of Radiofrequency Energy on Tissue

Electromagnetic radiation is propagated in the form of waves that may be considered as discrete particles called photons. The energy content of each photon is known from its frequency: $\Delta E = h\nu$, where E is the energy of the photon in electron volts, ν is the frequency of the photon in Hertz, and h is Planck's constant. The region of the electromagnetic spectrum related to biomedical NMR observation is roughly

between 1 and 100 MHz. The corresponding energy in one photon is 4×10^{-9} to 4×10^{-7} eV. The energy needed to eject an electron from a molecule is 10 to 25 eV. Medical x-rays and gamma sources emit photons above 10,000 eV, far above the usual ionizing potential. In contrast, NMR involves nonionizing radiation (129).

In biological systems, the principle effect of absorption of r.f. energy is the increased kinetic energy of the absorbing molecules, i.e., heating. This heating is due to vibration of dipolar molecules such as H_2O and protein, as well as ionic conduction. The amount of heating depends on the power and frequency of the r.f. energy as well as the tissue dimension and electrical properties (but fat less r.f. than muscle). Because of these factors, it is extremely difficult to precisely calculate the amount of energy deposited in a human (15,60).

The temperature increase after exposure to r.f. energy depends on the thermal conductivity and the effects of blood flow. The only significant mass of tissue in the body without flowing blood is the lens of the eye. Based on these theoretical considerations and experiments, the United States Food and Drug Administration (FDA) and the British National Radiological Protection Board (NRPB) have developed guidelines that limit patient exposure to r.f. energy (108,120).

6.2 Effects of Static and Switched Magnetic Field Gradients on Tissue

There was initially some concern that seizures or ventricular ectopy could be induced by NMR imaging because of rapidly shifting magnetic fields. To date, there are no reports of complications of imaging patients with a history of seizures or heart disease.

The major safety consideration in selecting patients for NMR studies is the presence of ferromagnetic materials within the body. Specifically, clips of the type used for intracranial aneurysms may be ferromagnetic and, therefore, subject to torque in a magnetic field (121). These patients are excluded from NMR imaging. A patient who works with metal should be questioned in detail about a history of metal fragments entering the eye. If there is a possibility of a retained fragment of metal in any tissue, he should not be imaged. The metals used for orthopedic implants, dental work, and surgical wire do not present a hazard (113,121). Generally, patients with prosthetic heart valves and pacemakers are not imaged, although this practice may be changing. If an NMR study is essential, then it should be discussed with the radiologist (127).

7. INDICATIONS FOR NMR IMAGING AND SPECTROSCOPY

Throughout this review of NMR principles, ^1H images have been selected to illustrate a particular aspect of NMR techniques. The favorable features of NMR imaging as a diagnostic technique should be summarized:

1. Soft tissue contrast is determined by multiple parameters and not simply x-ray or ultrasound density of the tissue. Contrast may be enhanced by selection of particular imaging parameters (pulse sequence, delay times).

2. Imaging is relatively available with excellent resolution in any plane (coronal, transverse, sagittal) relative to the patient's body. In the near future, any oblique imaging plane will be availble.

3. The method does not require contrast administration

4. No hazards are known (ionizing radiation is not used)

5. Signal is not attenuated by bone, fat, lung, or most implanted metals. Thus, imaging of patients with COPD or obese patients is not limited. Imaging of the posterior fossa is excellent.

In a nutshell, an NMR study should be considered for any disease modifying the structure of soft tissues. Almost any time you consider a CT study, you should consider NMR imaging. Generally, a radiologist with experience in NMR imaging and CT should be consulted about the incremental value of NMR.

NMR would probably be the preferred diagnostic procedure in many situations. There is a more limited set of conditions for which NMR imaging is superior to other techniques. NMR imaging should probably be obtained for evaluation of

1. Demyelinating disease
2. Suspected intracranial cystic abnormality
3. Posterior fossa lesion
4. Acoustic neuroma
5. Myelopathies (not radiculopathies)
6. Pediatric imaging
7. Soft tissue tumors of the musculoskeletal system
8. Pregnancy
9. Allergy to contrast or depressed renal function when contrast CT is needed
10. Hemangiomas of the liver

In contrast to NMR imaging, there is no currently clear clinical indication for NMR spectroscopy. It is probably helpful in the evaluation of inherited disorders of glycolysis in skeletal muscle, and for research in skeletal muscle metabolism.

The Future

As we have seen, NMR imaging and spectroscopy are simply two applications of the same phenomenon. What is impressive about this new technology is not, of course, the simple power to improve our characterization of a few diseases. What makes it impressive is the extraordinary flexibility and breadth of applications. It is by far the most sophisticated technique for imaging patients, and it is a part of routine medical practice where it is available. Even at this early stage it is clearly the diagnostic imaging technique of choice in certain situations. It is likely that as the technology matures clinically relevant information from imaging and spectroscopy will be simultaneously available. In the immediate future we may expect clinical ^{23}Na imaging (40,79,109), ^{1}H chemical shift imaging (137), advances in contrast agents, and improved flexibility of ^{1}H imaging techniques.

Acknowledgements

I thank Drs. Kenneth Maravilla, Ronald Peshock, and Jeff Weinreb for helpful discussion and for kindly providing the clinical images in this review. I am grateful to Nancy Dickey for her expert help in preparing this review.

REFERENCES

1. Ackerman JJH, Grove TH, Wong GG, Gadian DG, Radda GK (1980). Mapping of metabolites in whole animals by ^{31}P NMR using surface coils. Nature 283: 167.

2. Adey WR (1981). Tissue interactions with nonionizing electromagnetic fields. Physiol Rev 61: 435.

3. Alger JR, Shulman RG (1984). Metabolic applications of high resolution ^{13}C nuclear magnetic resonance spectroscopy. Br Med Bull 40: 160.

4. Andrew ER (1971). Magnetic resonance discovery celebrated. Nature 233: 374.

5. Andrew ER (1984). A historical review of NMR and its clinical applications. Brit Med Bull 40: 115.

6. Arnold DL, Matthews PM, Radda GK (1983). Metabolic recovery after exercise and the assessment of mitochondrial function in vivo in human skeletal muscle by means of ^{31}P NMR. J Magn Res Med. In press.

7. Arnold DL, Bore P, Radda G, Styles P. Taylor D (1984). Excessive intracellular acidosis of skeletal muscle on exercise in a patient with a post-viral exhaustion-fatigue syndrome. Lancet ii: 1367.

8. Balaban RS, Gadian DG, Radda GK (1981). A phosphorus nuclear magnetic resonance study of the rat kidney in vivo. Kidney International 20: 575.

9. Beall PT, Hazelwood CF, Rao PN (1976). Nuclear magnetic resonance patterns of intracellular water as a function of HeLa cell cycle. Science 192: 904.

10. Beall PT, Asch BB, Chang D, Medina D, Hazlewood CF (1980). Distinction of normal, preneoplastic, and neoplastic mouse primary cell cultures by water nuclear magnetic resonance relaxation times. J Natl Cancer Inst 64: 335.

11. Beischer DE (1962). Human tolerance to magnetic fields. Astronautics 7: 24.

12. Beischer DE, Knepton JC (1964). Influence of strong magnetic fields on the electrocardiogram of squirrel monkeys. Aerospace med 35: 939.

13. Bilaniak LT (1984). Magnetic resonance imaging of pituitary lesions. Radiology 153: 415.

14. Bloch F, Hansen WW, Packard ME (1946). Nuclear induction. Phys Rev 69: 127.

15. Bottomley PA, Edelstein WA (1981). Power deposition in whole-body NMR imaging. Med Phys 8: 510.

16. Bottomley PA, Hart HR, Edelstein WA, et al. (1983). NMR imaging/spectroscopy system to study both anatomy and metabolism. Lancet ii: 273.

17. Bradley WG (1984). Comparison of CT and MR in 400 patients with suspected disease of the brain and cervical spinal cord.

18. Bradley WG, Waluch V (1985). Blood flow: magnetic resonance imaging. Radiology 154: 443.

19. Brady JJ, Goldman MR, Pykett IL, Buonanno FS, Kisler JP, Newhouse JH, Burt CT, Hinshaw WS, Pohost GM (1982). Proton nuclear magnetic resonance imaging of regionally ischemic canine hearts: effect of paramagnetic proton signal enhancement. Radiology 144: 343.

20. Brasch RC (1983). Work in progress: Methods of contrast enhancement for NMR imaging and potential applications. A subject review. Radiology 147: 781.

21. Brooks RA, DeChiro G (1975). Theory of image reconstruction in computed tomography. Radiology 117: 561.

22. Budinger TF (1981). Nuclear magnetic resonance (NMR) in vivo studies: Known thresholds for health effects. J Comput Assist Tomogr 5: 800.

23. Budinger TF, Lauterbur PC (1984). Nuclear magnetic resonance technology for medical studies. Science 226: 288.

24. Burt CT, Cohen SM, Barany M (1979). Analysis of intact tissue with ^{31}P NMR. Ann Rev Biophys Bioeng 8: 1.

25. Cady EB, Dawson JM, Hope PL, et al. (1983). Non-invasive investigation of cerebral metabolism in newborn infants by phorphorus nuclear magnetic resonance spectroscopy. Lancet i: 1059.

26. Carr DH, et al. (1984). Gd DTPA as a contrast agent in MRI. Am J Radiology 143: 215.

27. Chance B, Eleff S, Leigh JS Jr, Sokolow D, Sapega A (1981). Mitochondrial regulation of phosphocreatine/inorganic phosphate ratios in exercising human muscle: A gated ^{31}P NMR study. Proc Natl Acad Sci USA 78: 6714.

28. Chance B, Eleff F, Bank W, Leigh JF Jr, Warnell R (1982). P^{31} NMR studies of control of mitochondrial function in phosphofrucktokinase deficient human skeletal muscle. Proc Natl Acad Sci USA 79: 7714.

29. Clegg JS (1981). Metabolic consequences of the extent and disposition of the aqueous intracelluar environment. J Exp Zool 215: 303.

30. Cooke P, Morris PG (1981). The effects of NMR exposure on living organisms: II. A genetic study of human lymphocytes. Br J Radiol 54: 622.

31. Cresshull I, Dawson MJ, Edwards RHT, et al. (1981). Human muscle analysed by ^{31}P nuclear magnetic resonance in intact subjects. Proc J Physiol 317: 18P.

32. Crooks LE et al. (1985). Thin-slice definition in magnetic resonance imaging. Radiology 154: 463.

33. Crooks LE, Hoenninger JC, Arakawa M, et al. (1980). Tomography of hydrogen with nuclear magnetic resonance. Radiology 136: 701.

34. Crooks LE, Arakawa M, Hoenningis J, et al. (1982). Nuclear magnetic resonance: whole body imager operating at 3.5 K gauss. Radiology 143: 169.

35. Crooks LE, Mills CM, David PL, et al. (1982). Visualization of cerebral and vascular abnormalities by NMR imaging: The effects of imaging parameters on contrast. Radiology 144: 843.

36. Damadian R (1971). Tumor detection by nuclear magnetic resonance. Science 171: 1151.

37. Damadian R, Zaner K, Hor D, et al. (1974). Human tumors detected by NMR. Proc Natl Acad Sci 71: 1471.

38. Damadian R, Goldsmith M, Minkoff L (1977). NMR in cancer: Fonar image of the live human body. Physiol Chem Phys 97.

39. Davis PL, Crooks L, Arakawa M, McRee R, Kaufman L, Margulis AR (1981). Potential hazards in NMR imaging: heating effects of changing magnetic fields and RF fields in small metallic implants. AJR 137: 857.

40. Delayre J, Ingwall J, Malloy C, Fossel E (1981). Gated sodium 23 nuclear magnetic resonance images of an isolated perfused working rat heart. Science 212: 935.

41. Doyle FH, Gore JC, Pennock JM, et al. (1981). Imaging of the brain by nuclear magnetic resonance. Lancet ii: 53.

42. Doyle M, Rzedzian R, Mansfield P, Coupland RE (1983). Dynamic NMR cardiac imaging in a piglet. Br J Radiol 56: 925.

43. Easterly CB (1982). Cardiovascular risk from exposure to static magnetic fields. Am Ind Hyg Assoc J 43: 533.

44. Edelstein WA, Bottomley PA, Hart HR, Smith LS (1983). Signal, noise and contrast in nuclear magnetic resonance (NMR) imaging. J Comput Assist Tomogr 7: 391.

45. Edelstein WA, Bottomley PA (1984). Magnetic resonance without nuclei. Radiology 152: 237.

46. Edelstein WA, Hutchison JMS, Johnson G, Redpath T (1980). Spin warp NMR imaging and applications to human whole-body imaging. Phys Med Biol 25: 751.

47. Edwards RHT, Wilkie DR, Dawson JM, Gordon RE, Shaw D (1982). Clinical use of nuclear magnetic resonance in the investigation of myopathy. Lancet ii: 725.

48. Eggleston JC, Saryan LA, Czeisler JL, et al. (1973). NMR studies of several experimental and human malignant tumors. Cancer Res 33: 2156.

49. Eiselein JE, Boutell HM, Biggs MW (1961). Biological effects of magnetic fields -- negative results. Aerospace Med 32: 383.

50. Ernst RR, Anderson WA (1966). Application of Fourier transform spectroscopy to magnetic resonance. Rev Sci Instrum 37: 93.

51. Fardon JC, Poydock ME Sr, Basulto G (1966). Effect of magnetic fields on the respiration of malignant, embryonic and adult tissue. Nature 211: 433.

52. Farrar TC, Becker ED (1976). Pulse and Fourier Transform NMR. New York: Academic Press.

53. Flaherty JT, Weisfeldt ML, Bulkley BH, Gardner TJ, Gott VL, Jacobus WE (1982). Mechanisms of ischemic myocardial cell damage assessed by phosphorus 31 NMR. Circulation 31: 561.

54. Fletcher BG, Jacobstein MD, Nelson AD, Riemenschneider TA, Alfidi RJ (1984). Gated magnetic resonance imaging of congenital cardiac malformations. Radiology 150: 137.

55. Frank JA, Feiler MA, House WV, Lauterbur PC, Jacobson MJ (1976). Measurement of proton nuclear magnetic longitudinal relaxation times and water content in infarcted canine myocardium and induced pulmonary injury. Clin Res 24: 217A (abstract).

56. Friedman H, Carey RF (1969). The effects of magnetic fields upon rabbit brains. Physiol Rev 4: 539.

57. Fukushima E, Roeder SB (1981). Experimental Pulse NMR: A Nuts and Bolts Approach. Reading: Addison-Wesley.

58. Gabillard R (1952). A steady state transient technique in nuclear resonance. Phys Rev 85: 694.

59. Gadian DG (1982). Nuclear Magnetic Resonance Application to Living Systems. Oxford: Clarendon Press.

60. Gadian DG, Robinson FN (1979). Radiofrequency losses in NMR experiments on electrically conducting samples. J Magn Reson 34: 449.

61. Gadian DG, Radda GK, Ross BD, et al. (1981). Examination of a myopathy by phosphorus NMR. Lancet i: 744.

62. Gadian DG, Radda GK (1981). NMR studies of tissue metabolism. Ann Rev Biochem 50: 69.

63. Garlick PB, Radda GK, Seeley PJ (1979). Studies of acidosis in the ischemic heart by phosphorus nuclear magnetic resonance. Biochem J 184: 547.

64. Garroway AN, Grannell PK, Mansfield P (1974). Image formation in NMR by a selective irradiative process. J Phys[C] 7: 457.

65. George CR, et al. (1984). Magnetic resonance signal intensity patterns obtained from continuous and pulsatile flow models. Radiology 151: 421.

66. Goldman MR, Brady TJ, Pykett IL, et al. (1982). Quantification of experimental myocardial infarction using NMR imaging and paramagnetic ion contrast enhancement in excised canine hearts. Circulation 66: 1012.

67. Gordon RE, Hanley PE, Shaw E, et al. (1980). Localisation of metabolites in animals using ^{31}P "topical magnetic resonance". Nature 287: 736.

68. Gordon RE, Hanley PE, Shaw D (1982). Topical magnetic resonance. Progress in Nuclear Magnetic Resonance Spectroscopy. 15: 1.

69. Gupta RK, Benovic JL, Rose ZB (1978). The determination of the free Mg^{++} level in the human red cell by ^{31}P NMR. J Biol Chem 253: 6172.

70. Haase A, Malloy C, Radda GK (1983). Spatial localisation of high resolution ^{31}P spectra with surface coils. J Magn Reson 55: 164.

71. Haberditzl W (1967). Enzyme activity in high magnetic fields. Nature 213: 72.

72. Haselgrove JC, Subramanian VH, Leigh JS, Gyulai L, and Chance B (1983). In vivo one-dimensional imaging of phosphorous metabolites by phosphorous-31 NMR. Science 220: 1170.

73. Hawkes RC, Holland GN, Moore WS, Roebuck EJ, Worthington BS (1981). Nuclear magnetic resonance tomography of the normal heart. J Comp Asst Tomo 5: 605.

74. Hazlewood CF, Nichols BL (1969). An NMR study of skeletal muscle: changes in water structure with normal development. Physiologist 12:251.

75. Herfkens R, David P, Crooks L, et al. (1981). NMR imaging of the abnormal live rat and correlations with tissue characteristics. Radiology 141: 211.

76. Herfkens RJ, Higgins CB, Hricak H, et al. (1983). Nuclear magnetic resonance imaging of the cardiovascular system: Normal and pathologic findings. Radiology 147: 749.

77. Hinshaw WS (1976). Image formation by nuclear magnetic resonance: The sensitive point method. J Appl Physiol 47: 3709.

78. Higgins CB, Herfkens R, Lipton MJ, et al. (1983). NMR imaging of acute myocardial infarction in dogs: alterations in magnetic relaxation times. Am J Cardiol 52: 184.

79. Hilal SK, Mohr J, Tatemichi T, et al. (1985). Sodium and proton NMR imaging in acute stroke. Stroke 16: 151 (abstract).

80. Hollis DP, Saryan LA, Eggleston JC, et al. (1975). NMR studies of cancer. J Natl Cancer Inst 54: 1469.

81. Hoult DI, Busby SJW, Gadian DG, Radda GK, Richards RE, Seeley PJ (1974). Observation of tissue metabolites using ^{31}P nuclear magnetic resonance. Nature 252: 285.

82. Hoult DI, Richards RE (1976). The signal-to-noise ratio of the nuclear magnetic resonance experiment. J Mag Res 24: 71.

83. Hoult DI (1978). The NMR receiver: a description and analysis of design. Prog NMR Spectry 12: 41.

84. Hoult DI (1979). Rotating frame zeugmatography. J Magn Reson 33: 183.

85. Hoult DI (1984). NMR imaging techniques. Brit Med Bull 40: 132.

86. Hutchison JMS, Edelstein WA, Johnson E (1980). A whole-body NMR imaging machine. J Phys E Sci Instrum 13: 947

87. Iles RA, Stevens AN, Griffiths JR (1982). NMR studies of metabolites in living tissue. Prog in NMR Spectroscopy 15: 49.

88. Inch WR, McCredit JA, Knispel RR, et al. (1974). Water content and proton spin relaxation times for malignant and non-malignant tissues from mice and humans. J Natl Cancer Inst 52: 353.

89. Johnston DL, et al. (1985). Assessment of myocardial ischemia with proton magnetic resonance: effects of three hour coronary occlusion with and without reflow. Circulation 71: 595.

90. Kaufman L, Crooks L, Sheldon P, et al. (1983). The potential impact of nuclear magnetic resonance imaging on cardiovascular diagnosis. Circulation 67: 251.

91. Kaufman L, Crooks LE, Margulis AR (Eds) (1981). Nuclear Magnetic Resonance Imaging in Medicine. New York: Igaku-Shoin.

92. Kingsley DPE (1985). Acoustic neuromas: evaluation by magnetic resonance imaging. Am J Neuroradiol 6: 1.

93. Kiricuta IC, Simplaceanu V (1975). Tissue water content and nuclear magnetic resonance in normal and tumor tissue. Cancer Research 35: 1164.

94. Kolata GB (1976). Water structure and ion binding: a role in cell physiology? Science 192: 1220.

95. Kumar A, Welti D, Ernst RR (1975). NMR Fourier Zeugmatography. J Magn Reson 18: 69.

96. Kurtz D, Dwyer A (1984). Isosignal contours and signal gradients as an aid to choosing MR imaging techniques. J Comp Asst Tomo 8: 819.

97. Kurtz KD, Zipp A (1977). Water in biological systems. N Engl J Med 297: 262.

98. Lauterbur PC (1973). Image formation by induced local interactions: examples employing NMR. Nature 242: 190.

99. Levengood WC (1966). Cytogenetic variations induced with a magnetic probe. Nature 209: 1009.

100. Liburdy RP (1982). Carcinogenesis and exposure to electrical and magnetic fields. N Engl J Med 307: 1402.

101. Ling GN, Tucker M (1980). Nuclear magnetic resonance relaxation and water contents in normal mouse and rat tissues and in cancer cells. J Natl Cancer Inst 64: 1199.

102. Malinin GI, Gregory WD, Morelli L, et al. (1976). Evidence of morphological and physiological transformation of mammalian cells by strong magnetic fields. Science 184: 844.

103. Malloy C, Matthews P, Smith M, Radda GK (1985). In vivo ^{31}P NMR study of the regional metabolic responses to cardiac ischemia. Advances in Myocardiology, Vol. 6. In press.

104. Malloy CR, Sherry AD, Nunnally RC (1985). ^{13}C NMR measurement of flux through alanine aminotransferase by inversion and saturation transfer methods. J Magn Reson. In press.

105. Mansfield P, Maudsley AA (1977). Medical imaging by NMR. Br J Radiol 50: 188.

106. Mansfield P, Pykett IL (1978). Biological and medical imaging by NMR. J Magn Reson 29: 355.

107. Mansfield P, Morris PG (1982). NMR imaging in biomedicine. In Advances in Magnetic Resonance, Waugh JS (Ed), Suppl. 2. New York: Academic Press.

108. Margulis AR, Higgins CB, Kaufman L, Crooks LE (1983). Clinical Magnetic Resonance Imaging. San Francisco: University of California Printing Department.

109. Maudsley AA, Hilal SK (1984). Biological aspects of sodium 23 imaging. Brit Med Bull 40: 165.

110. Maudsley AA, Hilal SK, Simon HE, Wittekoek S (1984). In vivo spectroscopic imaging with P-31. Radiology 153: 745.

111. McNamara MT, et al. (1985). Detection and characterization of acute myocardial infarction in man with use of gated magnetic resonance. Circulation 71: 717.

112. Meaney TF (1984). Magnetic resonance without nuclear. Radiology 150: 277.

113. Mechlin M, Thickman D, Kressel HR, Gefter W, Joseph P (1984). Magnetic resonance imaging of post operative patients with metallic implants. Am J Radiol 143: 1281.

114. Medina D, Hazlewood CF, Cleveland G, et al. (1975). NMR studies on human breast dysplasias and neoplasms. J Natl Cancer Inst 54: 813.

115. Michael LH, Seitz P, McMillan-Wood J, et al. (1980). Mitochondrial water in myocardial ischemia: investigation with nuclear magnetic resonance. Science 208: 1267.

116. Milham S (1982). Mortality from leukemia in workers exposed to electrical and magnetic fields. N Engl J Med 307: 249.

117. Moon RB, Richards JH (1973). Determination of intracellular pH by 31 P magnetic resonance. J Biol Chem 248: 7276.

118. Mountford CE, et al. (1984). High resolution proton nuclear magnetic resonance analysis of metastatic cancer cells. Science 226: 1415.

119. Nahas GG, Boccalon H, Berryer P, Wagner B (1975). Effects in rodents of a 1 month exposure to magnetic fields (200-1200 Gause). Aviat Space and Environ Med 46: 1161.

120. National Radiological Protection Board (1984). Advice on acceptable limits of exposure to nuclear magnetic resonance clinical imaging. Radiography 50: 220.

121. New PFJ, Rosen BR, Brady TJ, et al. (1983). Potential hazards and artifacts of ferromagnetic and non-ferromagnetic surgical and dental materials and devices in nuclear magnetic resonance imaging. Radiology 147: 139.

122. Newman RJ, Bore PJ, Chan L, et al. (1982). Nuclear magnetic resonance studies of forearm muscle in patients with Duchenne dystrophy. Br J Med 284: 1072.

123. Nunnally RL, Hollis DP (1979). ATP compartmentation in living heart: a phosphorus NMR saturation transfer study. Biochemistry 18: 3642.

124. Ordidge RJ, Mansfield P (1981). Rapid biomedical imaging by NMR. Br J Rad 54: 850.

125. Ortendahl DA, et al. (1984). Analytical tools for magnetic resonance imaging. Radiology 153: 479.

126. Partain CL, et al (Eds) (1983). Nuclear Magnetic Resonance (NMR) Imaging. Philadelphia: W.B. Saunders.

127. Pavlicek W, Geisinger M, Castle L, et al. (1983). The effects of nuclear magnetic resonance on patients with cardiac pacemakers. Radiology 147: 149.

128. Pflugfelder PW, et al. (1985). Early detection of canine myocardial infarction by magnetic resonance imaging in vivo. Circulation 71: 587.

129. Pollard EC (1969). The biological action of ionizing radiation. Am Sci 57: 206.

130. Purcell EM, Torrey HC, Pound RV (1946). Resonance absorption by nuclear magnetic moments in a solid. Phys Rev 69: 37.

131. Pykett IL, Newhouse JH, Buonanno FS, et al. (1982). Principles of nuclear magnetic resonance imaging. Radiology 143: 157.

132. Pykett IL (1982). NMR imaging in medicine. Sci Am 246: 78.

133. Radda GK, Bore P, Rajagopalan B (1984). Clinical aspects of NMR spectroscopy. Brit Med Bull 40: 155.

134. Radda GK, Seeley PJ (1979). Recent studies on cellular metabolism by nuclear magnetic resonance. Ann Rev Physiol 41: 749.

135. Radda GK, Bore PJ, Gadian DG, et al. (1982). ^{31}P NMR examination of two patients with NADH-CoQ reductase deficiency. Nature 295: 608.

136. Ratner AV, Okada RD, Newell JB, Pohost GM (1985). The relationship between proton nuclear magnetic resonance relaxation parameter and myocardial perfusion with acute coronary arterial occlusion and reperfusion. Circulation 71: 823.

137. Rosen BR, et al. (1985). Proton chemical shift imaging: an evaluation of its clinical potential using an in vivo fatty liver model. Radiology 154: 469.

138. Ross BD, Radda GK, Gadian DG, et al. (1981). Examination of a case of suspected McArdle's syndrome by ^{31}P NMR. New Engl J Med 304: 1338.

139. Saunders RD, Orr JS (1983). Biologic effect of NMR. In Nuclear Magnetic Resonance (NMR) Imaging, Partain CL et al (Eds), Chap. 28. Philadelphia: W.B. Saunders.

140. Shaw D (1976). Fourier transform nuclear magnetic resonance spectroscopy. Amsterdam: Elsevier.

141. Shulman RG (1983). NMR spectroscopy of living cells. Sci Am 248: 86.

142. Shulman GI, Alger JR, Prichard JW, Shulman RG (1984). Nuclear magnetic resonance spectroscopy in diagnostic and investigative medicine. J Clin Invest 74: 1127.

143. Shoubridge EA, Briggs RW, Radda GK (1982). ^{31}P NMR saturation transfer measurements of the steady state rates of creatine kinase and ATP synthetase in the rat brain. FEBS Lett 140: 288.

144. Singer JR, Crooks LE (1983). NMR blood flow measurements in the human brain. Science 221: 654.

145. Singer JR (1978). NMR diffusion and flow measurements and an introduction to spin phase graphing. J Phys E 11: 281.

146. Slutsky RA, Brown JJ, Peck WW, et al. (1984). The effects of transient coronary ischemia and reperfusion on myocardial edema formation and in vitro magnetic relaxation times. J Am Coll Cardiol 3: 1454.

147. Taylor DJ, Bore PJ, Styles P, et al. (1983). Bioenergetics of intact human muscle: a ^{31}P nuclear magnetic resonance study. Mol Biol Med 1: 77.

148. Thomas A, Morris PG (1981). The effects of NMR exposure on living organisms: I. A microbial assay. Br J Radiol 54: 615.

149. Weisman ID, Bennett LH, Maxwell LR, et al. (1972). Recognition of cancer in vitro by NMR. Science 178: 1288.

150. Welch K, Helpern J, Robertson W, Ewing J (1985). ^{31}P topical magnetic resonance measurements of high energy phosphates of normal and infarcted human brain. Stroke 16: 151 (abstract).

151. Wesbey G, Higgins CB, Lanzer P, et al. (1984). Imaging and characterization of acute MI in vivo by gated NMR. Circulation 69: 125.

152. Wesbey GE, et al. (1984). Effects of Gd DTPA on the magnetic relaxation times of normal and infarcted myocardium. Radiology 153: 165.

153. Whalen D, et al. (1974). Effect of a transient period of ischemia on myocardial cells. I. Effects on cell volume regulation. Am J Pathol 74: 381.

154. Williams ES, Kaplan JI, Thatcher F, Zimmerman G, Knoebel SB (1980). Prolongation of proton spin lattice relaxation times in regionally ischemic tissue from dog hearts. J Nucl Med 21: 445.

155. Wolff S, Crooks LE, Brown P, et al. (1980). Tests for DNA and chromosomal damage induced by nuclear magnetic resonance imaging. Radiology 136: 707.

156. Wright WE, Peters JM, Mack TM (1982). Leukemia in workers exposed to electrical and magnetic fields. Lancet i: 1160.

157. Young IR, Hall AS, Pallis CA, et al. (1981). Nuclear magnetic resonance imaging of the brain in multiple sclerosis. Lancet ii: 1063.